Small Spirocyclic, Xanthene-Based Fluorescent Probes

Subjects: Biochemistry & Molecular Biology
Contributor: Sascha Keller

The use of fluorescent probes in a multitude of applications is still an expanding field. This review covers the recent progress made in small molecular, spirocyclic xanthene-based probes containing different heteroatoms (e.g., oxygen, silicon, carbon) in position 10′. After a short introduction, we will focus on applications like the interaction of probes with enzymes and targeted labeling of organelles and proteins, detection of small molecules, as well as their use in therapeutics or diagnostics and super-resolution microscopy. Furthermore, the last part will summarize recent advances in the synthesis and understanding of their structure–behavior relationship including novel computational approaches.

Keywords: rhodol ; rhodamine ; imaging ; fluorescent probes ; fluorescein ; xanthene-based ; spirocyclic

1. Introduction

Adolf von Bayer first synthesized fluorescein in 1871 from phthalic anhydride and resorcinol in the presence of zinc chloride [1]. Since then, fluorescein and its plethora of congeners manifested in a new and versatile branch of research [2]. Nowadays there are many different classes of fluorophores, ranging from large fluorescent proteins (i.e., green fluorescent protein (GFP), yellow fluorescent protein (YFP)) [3][4][5] over small fluorescent molecules (i.e., coumarins [6][7], naphtalimides [8][9][10], BODIPYs [11][12][13][14], cyanines [15][16] or fluoresceins/rhodamines [17][18][19][20]) to fluorescent quantum dots [21][22]. Three main classes exist: fluorescein (contains two phenol groups), rhodamine (contains two aniline groups), and rhodol (contains one phenol group and one aniline group) [23]. Commercialized fluorescein/rhodamine-based dyes (e.g., MitoTracker [24]) are being used daily in a vast amount of chemical, biological or medical research laboratories. These molecules are utilized to visualize and quantify a multitude of static or dynamic processes in living cells due to their high sensitivity, real-time detection, and non-destructive fast analysis [25][26][27]. The probes can target a variety of biological targets due to their structural adjustability [28][29][30][31][32]. Fluoresceins/rhodamines are specifically interesting because of their ability to form a non-fluorescent spirocyclic and a fluorescent open form which can be controlled by external triggers like pH, chelation, or an enzymatic reaction [33]. Furthermore, the ease of chemical modification, good water solubility, high stability and brightness makes them the most popular dyes used in fluorescence imaging. The main chromophore of fluorescein/rhodamine is its xanthene-core, which contains a bridging oxygen-atom in position 10′ (Scheme 1) [34][35]. This bridging atom rigidifies the structure to maximize the π-conjugation within the molecule and thus its fluorescence [19][36][37][38]. However, the absorption and emission of fluoresceins/rhodamines lie within the range of 500–600 nm, which limits their use in multicolor or in vivo imaging. The change of the bridging O-atom to other atoms (C, Si, P, Se, S, Ge, or N) shifts the molecules absorbance maxima to the near-infrared region (NIR) [39]. Many dyes have been developed that cover different parts of the spectrum [40].

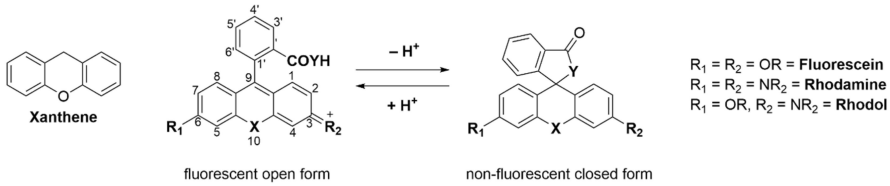

Scheme 1. Xanthene, the core-structure of fluorescein and the equilibrium of the open and the closed form of a spirocyclic dye. X = O, S, $Si(CH_3)_2$, $C(CH_3)_2$ and others; Y = O, NH.

Spirocyclic, xanthene-based probes usually have a hydroxy- or carboxy-moiety or other intramolecular nucleophiles at the 2′ position of a pendant aromatic ring at the C-9′-atom of the xanthene core (Scheme 1) [41][42]. This intramolecular nucleophilic-moiety attacks the sp_2-hybridized C-9′-atom and forms the colorless spirocyclic form. We previously determined the pH-value at which 50% of the molecules are present in the non-fluorescent form as the pK_{cycl} value [43]. Chemical modification of the xanthene core, intramolecular nucleophiles, and the pendant aromatic ring can significantly alter that value [44][45]. This pK_{cycl} value is especially important if the dye should be highly fluorescent at a certain pH, such

as the physiological pH of 7.4 for example. On the other hand, for high resolution microscopy it is important that the pK_{cycl} value is much lower, since only a tiny fraction should be fluorescent at a given time so single molecules can be detected [46][47].

Another advantage of these dyes is that they can be caged by reacting their aniline or phenol groups with, for example, moieties which are reactive towards biologically relevant molecules or proteins via ether, amide, or ester bonds. This caging alters the fluorescence behavior of the fluorophore turning it non-fluorescent and only after reaction with the desired target is its bright fluorescence restored [48][49][50]. This target-oriented fluorescence activation is what makes these dyes so interesting, as it often results in high signal-to-noise ratios because of little to no nonspecific activation. Targets can range from enzymes to small molecules, organelles, metal ions or simply the pH of the surrounding environment. Moreover, structural changes in the probe itself alter its spectroscopic properties, which allows for fine tuning of the excitation and emission wavelengths [51][52]. For example, many fluorescein/rhodamine analogues have been developed that contain a different heteroatom (e.g., Si, C, P, Se) than oxygen in the 10′-position, resulting in large shifts of their emission and excitation maxima and hence different colors [39][53]. These probes can then be used simultaneously, and different targets can be targeted at the same time. Furthermore, a shift to the near infrared (NIR) region allows deeper penetration of tissue, as well as less photodamage, given the lower energy of the light [54][55].

Several different signal-conversion mechanisms have been utilized. These include Förster resonance energy transfer (FRET) [53], intramolecular charge transfer (ICT) [56], photo-induced electron transfer (PeT) [57][58] and restriction of intramolecular motion (RIM) [59].

2. Applications

2.1. Enzyme Activation

The detection of enzymatic activity in living cells has become an important field of modern research [60]. Enzymes hold important roles in many physiological, pathological, and pharmacological processes. It is widely accepted that some enzymes are causally related to a variety of cancers. For example, γ-glutamyl-transpeptidase is expressed in high levels in several cancers, including liver, cervical and ovarian cancers [61][62][63][64]; enhanced enzymatic activities of alkaline phosphatase can be detected in some bone cancers [65]; β-galactosidase shows increased activity in primary ovarian cancers [66]. Localizing and determining the expression levels of these enzymes in live cancer cells is of great importance for diagnosing cancer in its early stages and for monitoring the efficacy of therapies. Enzymes specifically catalyze the conversion of certain substrates to their products. A probe bound to one of these substrates will remain non-fluorescent, but upon reaction with the desired enzyme, it will restore its fluorescence. These “turn-on”-probes can achieve high signal-to-noise ratios. In some cases, a linker between the substrate and the fluorophore is desired, to reduce steric hindrance with bulky fluorophores that could hinder the binding of the conjugated substrate into the active pocket of the enzyme [67]. Another approach is the use of non-substrate-based probes, which are bound to the inhibitors of enzymes or their natural ligands. The difficulty here lies in the fact that it is challenging to discriminate between bound and non-bound probes. Probes have been developed that turn fluorescent after binding to the protein of interest [68]. Since the molecule is bound to the enzyme, enzyme activation in real-time can be monitored and its activation and localization can be studied dynamically.

2.2. Organelle and Protein Labeling

The visualization of organelles plays an important role in biological sciences. Each organelle contains its own proteome, which is involved in its structural and functional properties [69]. Lysosomes, often referred to as the stomach of the cell, mitochondria, the powerhouse of the cell, and the cell nucleus are just some of the important organelles in cells. The targeting of specific organelles is of great interest; Mitochondria for instance play a critical role in several vital processes such as ATP production, central metabolism and apoptosis and a dysfunction is related to many diseases [70].

To target mitochondria and simultaneously produce a water-soluble always on probe Xiao and coworkers mimicked the spirolactam opening effect induced by metal-ions (Figure 1a, top) [71]. They incorporated a positive charge via a quarterly o-aminopyridine, that resembles the positive charge induced by bound metals (Figure 1a, middle) [72]. The probe o-RPM shows florescence at a broad pH range (pH 3.5–13.0) and also in aprotic solvents such as DCM, DMSO or acetonitrile. A pH titration of o-RPM and a range of similar control molecules (Figure 1a, bottom) showed that the controls were quenched at higher pH-values (pK_{cycl} 4.46–5.67), whereas the target molecule showed excellent stability over a broad pH range (Figure 1b). Mitochondria selectivity was confirmed by co-staining with Rhodamine 123, a commercial mitochondrion tracker.

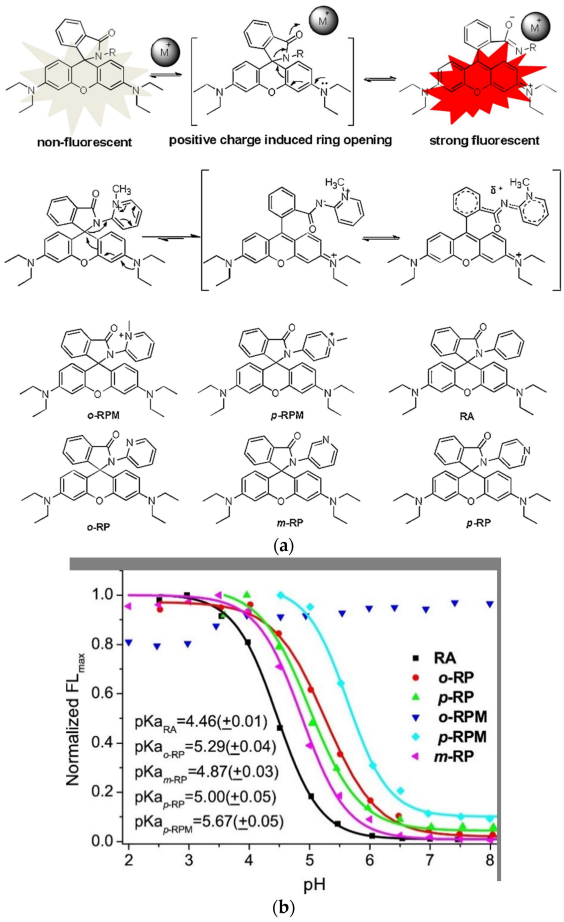

Figure 1. Acid resistant, always-on, mitochondria targeting probe: (**a**) (**top**) Metal ion induced ring-opening reaction of rhodamine spirolactam; (**middle**) Dominant structure of "always-on" rhodamine spirolactam **o-RPM**; (**bottom**) Structures of **o-RPM** and some rhodamine control spirolactams; (**b**) Normalized intensity at emission maximum vs various pH values in aqueous solutions of **o-RPM** and controls. Adapted with permission from [71].

2.3. Therapy and Diagnostics

Cancer is one of the major diseases that humanity is facing. Many therapies to cure or slow down its development have been developed and many of them include small molecule drugs [73][74]. One major issue with these drugs is that they tend to attack healthy cells as well. The most widely used anticancer drug is Cisplatin, which is also the only metal-based anticancer drug used clinically [75][76][77]. Even though it is widely used, it has toxic side effects, which led researchers to develop non-platinum metal anticancer drugs [78][79][80]. Nowadays several other transition metal complexes like iridium complexes that show anticancer activity have been developed [81][82][83][84][85][86]. However, half-sandwich iridium complexes for example suffer from unknown targets, unclear mechanisms and poor selectivity between cancer and normal cells [87][88]. One target of anti-cancer compounds are lysosomes, which are evolutionary conserved organelles that are thought to play a big role in the regulation of apoptosis [89][90]. To better understand and address the above-mentioned issues the group of Liu developed four rhodamine coordinated iridium complexes complex 1–complex 4 which show high anticancer activity (Figure 2a) [91].

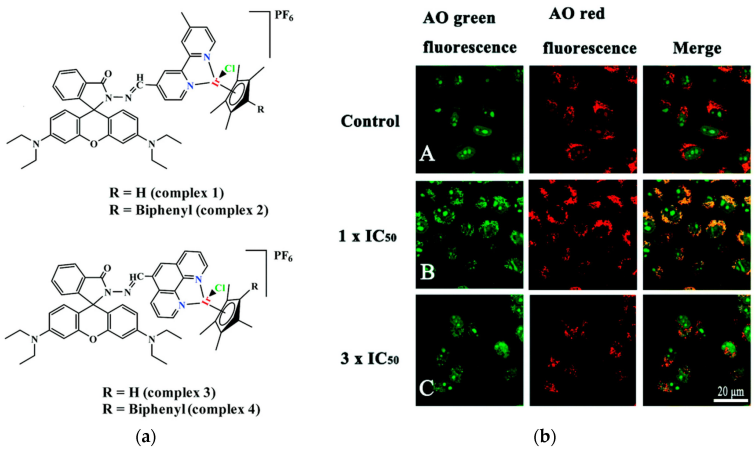

Figure 2. Ir-piano-stool anticancer drugs: (**a**) Structures of four iridium piano-stool rhodamine anticancer drugs; (**b**) Lysosomal membrane permeabilization in A549 cancer cells. A549 cells without (**A**), with 1 × IC_{50} (**B**) and 3 × IC_{50} (**C**) **complex 3** and then stained with AO. Adapted with permission from [91].

2.4. Small Molecule Detection

Biothiols, for example, are important antioxidants during oxidative stress or injury, serve as chelators for metals and act as essential signaling molecules. For example, glutathione (GSH) the most abundant non-protein biothiol, is involved among others in the maintenance of intracellular redox activities and signal transduction, proliferation, apoptosis, and gene regulation [92][93]. Its concentration ranges intracellularly from 1–10 mM and extracellularly from about 5–25 µM. Abnormal levels of biothiols are linked to several diseases, including cancer. Cysteine (Cys) for example is linked to liver damage, slow growth, or edema, while homocysteine (Hcy) is associated with cardiovascular and Alzheimer's disease, and H_2S is linked to colorectal cancer [94][95][96]. Given their importance in cell metabolism fluorescent probes have been developed to track the concentration of biothiols in real time with high sensitivity and selectivity [97].

However, that most probes lack discrimination between the different biothiols still presents a challenge. A novel glutathione selective near-infrared probe was developed by Quian and coworkers that could detect GSH over Cys and Hcy within 5 s by the naked eye [98]. Their system is based on a conjugate addition by a Knoevenagel reaction and intramolecular amino induced spirolactam opening (Figure 3). The chemosensor RhAN absorbs at 717 nm and emits at 739 nm with an increase of fluorescence of 90-fold after addition of GSH (20 mM), while other amino acids showed almost no increase in fluorescence.

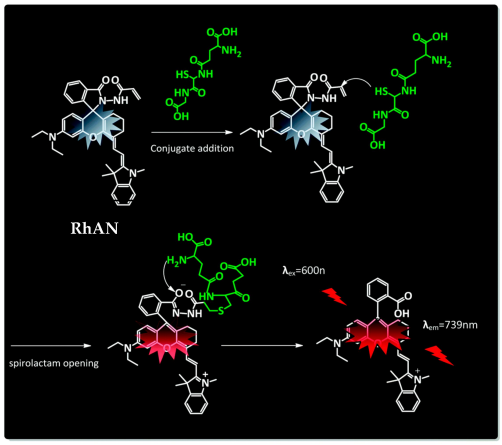

Figure 3. The possible mechanism of **RhAN** sensing toward GSH based on conjugate addition and intramolecular amino induced spirolactam opening. Adapted with permission from [98].

2.5. Super-Resolution Microscopy

Super-resolution microscopy, developed by Betzig, Hell and Moerner was awarded the Nobel Prize in 2014, and became a powerful tool to visualize cells [99][100][101]. Several recent techniques in super-resolution imaging made it possible to look beyond the diffraction-limit of about ≈200 nm in common microscopy. The developed techniques include stimulated emission depletion (STED) [102][103], photoactivated localization (PALM) [104][105], and stochastic optical reconstruction (STORM) [106][107]. These have been widely used to image biomacromolecules or subcellular organelles with sub-diffraction resolutions. The principle of super-resolution PALM imaging for example makes use of "dark" and "fluorescent" pair states of the fluorescent dyes. Due to a quick change between the open and closed form a blinking is observed, which enables the temporal and spatial separation of adjacent molecules. While photoactivatable fluorescent proteins and small molecular fluorophores are employed, rhodamines remain the main fluorophore used, due to their superior photostability. The group of Yang developed a nitroso-caged photoactivatable rhodamine for PALM super-resolution imaging of lysosomes [108]. Even though a variety of photo-cages have been developed, only o-nitrobenzyl groups and a few others are being utilized as PALM probes [109][110][111][112][113].

Dyes with photo cleavable o-nitrobenzyl groups, release toxic and highly colored o-nitrobenzaldehyde upon cleavage. The newly reported probe NOR535 on the other hand is non-fluorescent and upon irradiation with UV light (405 nm) only endogenous and biocompatible nitric oxide is produced (Figure 4a). Two morpholine moieties were introduced to target lysosomes. After the nitric oxide was cleaved the resulting probe showed slight fluorescence (λ_{exc} = 520 nm, λ_{em} = 550 nm, Φ = 0.09), probably due to a PET quenching effect of the morpholines. Upon protonation (as mentioned before lysosomes are acidic organelles), however, bright fluorescence with a blue-shifted excitation and emission wavelengths was obtained (λ_{exc} = 510 nm, λ_{em} = 535 nm, Φ = 0.97). The photo-activatable probe was utilized in HeLa cells and

colocalization with Lysotracker Red confirmed the selectivity for lysosomes. Super resolution PALM imaging of lysosomes in HeLa cells by a total internal refraction fluorescence microscope (TIRFM) showed reconstructed super resolution images with a detailed lysosomal morphology (Figure 4b). The transverse profiles of a single lysosome revealed a width of 86.8 nm. The number of mean photons emitted was ≈577 with a good localization precision of 14.3 nm.

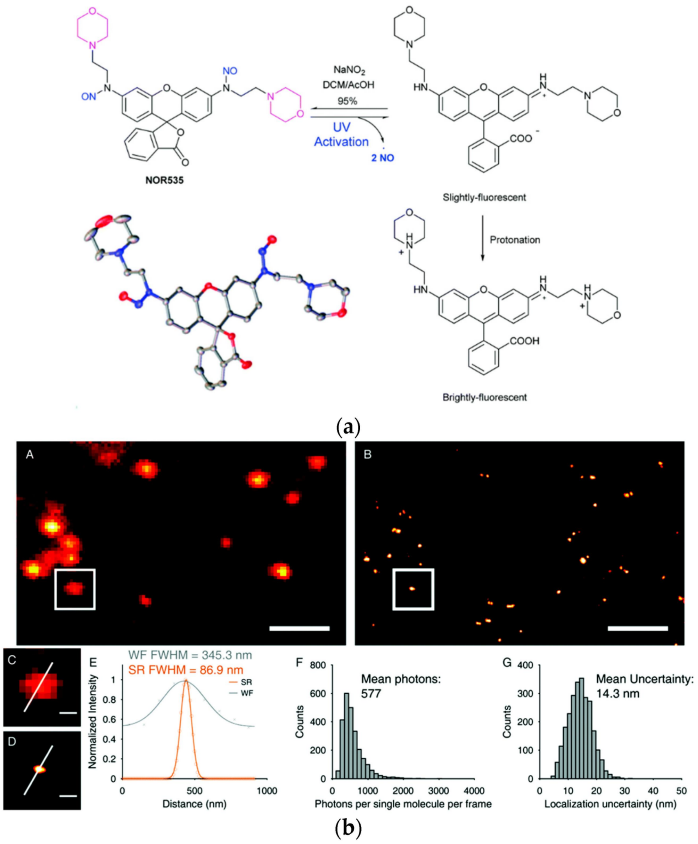

Figure 4. Biocompatible photo-caging strategy: (**a**) Structure, crystal structure and sensing mechanism of **NOR535**; (**b**) **NOR535** super-resolution imaging of lysosomes in live HeLa cells. Wide-field image (**A**) and PALM image (**B**) of the lysosomes; (**C**,**D**) Enlarged maps of the boxed areas of images A and B, respectively, showing a single lysosome. (**E**) Transverse profile of a single lysosome along the white line in C and D. (**F**) Histograms of the number of photons per single-molecule event. (**G**) Histograms of the localization precision. Adapted with permission from [108]. Scale bars = 2 µm (**A**,**B**), 300 nm (**C**,**D**).

3. Synthesis and Structural Aspects

Even though xanthene-based dyes have been known and investigated for about 150 years, their structure-function properties are still not completely understood. Deactivation pathways, solubility and biocompatibility issues, solvent effects, fine tuning of spectroscopic properties and related difficult syntheses are just a few problems. An interesting enhancement of the biocompatibility of rhodamine probes by a neighboring group effect was investigated by Lukinavičius and coworkers [114]. Fluorescent probes are often bound through a linker to a small molecular ligand, that allows targeting the protein of interest. The linker and the fluorophore contribute largely to the final properties of the probe. The result is often a reduced cell permeability or off-targeting [53][115]. Spirocyclic probes are present in their open, zwitterionic and thus more hydrophilic form, or in their spirocyclic hydrophobic form, which shows better cell-permeability [116][117]. Several ways have been investigated to favor the spirocyclic form and hence increase the cell-permeability [118][119][120][121]. The methods include introducing electron-withdrawing groups into the xanthene core or into the benzoic acid substituent. These changes result in a bulkier core structure and alter the physicochemical properties of the dyes. By exploiting the neighboring group effect (NGE), an effect where for example two neighboring carboxy groups can influence each other via steric, electrostatic, or H-bond interactions, the group managed to develop probes with outstanding cell permeability without changing their spectroscopic properties [122]. In contrast to the well-known 5′/6′-carboxyrhodamines the existence of their 4′-isomers was debated for a long time due to synthetic challenges arising from steric hinderance and the altered reactivity of adjacent carbonyl groups related to the ortho-effect [19].

4. Computational Approaches

Even though there are plenty of probes available and guidelines on how to fine tune and rationally design the pK_{cycl} value of spirocyclic probes, it is still mostly a trial-and-error approach to end up with a molecule with the desired properties. Synthesis is often time consuming and involves many steps to introduce a certain group into a molecule which often must be already present in the starting materials. Computational chemistry has become a crucial part of today's research and it can help to predict equilibrium constants of spirocyclization of novel molecules as our group has shown recently for hydroxymethyl rhodamines (HMR) [44]. This might help to revolutionize design strategies and hence eliminate time-consuming synthesis of multiple candidates. The equilibrium of the open and the closed form is pH-dependent and the pK_{cycl} values of known HMR derivatives were used to quantum chemically predict novel probes. Assuming that only four species (open forms under acidic O_A and basic conditions O_B and closed forms under acidic C_A and basic C_B conditions) were involved in this equilibrium the pK_{cycl} value can be interpreted as the pH value at which the concentration of the open forms (O_A + O_B) is equal to that of the closed forms (C_A + C_B) (Figure 5A,B). This leads to the equation in Figure 5C which can be used to predict pK_{cycl} values by quantum chemically estimating the difference in free energy ΔG between the open form and the closed form. The equilibrium constants K_{aOH} and K_{aNH} can be replaced by reported pK_a values of similar structures (benzyl alcohol, $K_{aOH} = 10^{-15.4}$; aniline, $K_{aNH} = 10^{-4.6}$; N,N-dimethylaniline, $K_{aNH} = 10^{-4.9}$).The calculations were performed at the B3LYP/6-31G(d) level with water included in the PCM model. We found that it is crucial for accurate calculations to introduce first shell water molecules in the calculations, and that a three-water bridge between the nucleophilic hydroxymethyl group and the amino groups of the xanthene ring gave results in very good agreement with previously reported values of known rhodamine probes. These results are interesting, since the proton moves from the nucleophile to the amino group during the spirocyclization reaction. The activation free energy of this reaction of HMTMR was thus estimated to be 28.7 kJ mol^{-1} by IRC calculations which suggests the reaction can proceed spontaneously at room temperature [123]. Next, we calculated pK_{cycl} values of molecules bearing F, Me, CF_3 or H moieties in positions 3′, 4′, 5′ and 6′ of the benzyl ring, that have never been synthesized before. After synthesizing a few of these structures, their measured pK_{cycl} values were in good agreement with their predicted values. The trend of the introduced groups suggests a strong impact on lowering the pK_{cycl} value by substituents on position 3, regardless of their electron-donating- or withdrawing effects. The bulkiness of the moieties next to the attacking nucleophile seems to play a bigger role.

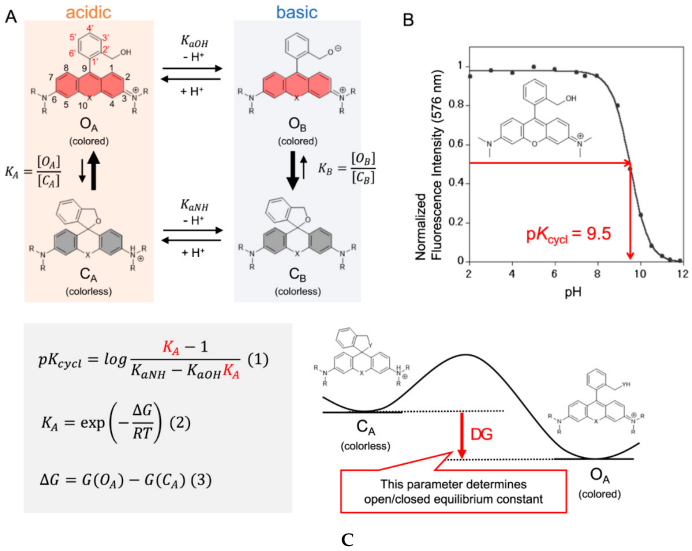

Figure 5. Intramolecular spirocyclization of HMR derivatives. (**A**) Acid–base equilibrium of HMR derivatives; (**B**) Correlation between pH and normalized fluorescence intensity of HMTMR; (**C**) Formula for pK_{cycl} based on statistical mechanics and the visualization of ΔG. Adapted with permission from [44].

5. Conclusions and Perspective

In this review, we summarize the research progress on small, spirocyclic xanthene-based fluorescent probes within the last three years. For 150 years spirocyclic xanthene dyes have become an essential tool for modern research. This review covered only a fraction of possible applications and recent publications in the field. Even though these probes have been used for a long time, many uncertainties remain. Researchers like Lavis, Lukinavičius, Johnsson, and Hell have helped to understand and cope with effects such as photobluing, cell permeability, and how to fine tune probes to hold the best possible properties. Computational chemistry is by far no new technology, but it only recently became of great interest for predicting suitable candidates without the need for tedious syntheses,as shown by us and the Liu group. This might lead to novel probes that will perform their task more efficiently, resulting in brighter,

more precisely located, less toxic, and at higher wavelengths absorbing fluorophores. With nitrogen and phosphate, almost all possible bridging atoms have already been introduced, but this may not be the end of their optimization as different oxidation states or bound groups might also have a great influence. A combination of these new findings may facilitate the development of probes that can easily be used in vivo, which still remains an ongoing challenge.

References

1. Baeyer, A. Ueber eine neue Klasse von Farbstoffen. Eur. J. Inorg. Chem. 1871, 4, 555–558.
2. Lavis, L.D. Teaching Old Dyes New Tricks: Biological Probes Built from Fluoresceins and Rhodamines. Annu. Rev. Biochem. 2017, 86, 825–843.
3. Tsien, R.Y. The Green Fluorescent Protein. Annu. Rev. Biochem. 1998, 67, 509–544.
4. Rodriguez, E.A.; Campbell, R.E.; Lin, J.Y.; Lin, M.Z.; Miyawaki, A.; Palmer, A.E.; Shu, X.; Zhang, J.; Tsien, R.Y. The Growing and Glowing Toolbox of Fluorescent and Photoactive Proteins. Trends Biochem. Sci. 2017, 42, 111–129.
5. Chudakov, D.M.; Matz, M.V.; Lukyanov, S.; Lukyanov, K.A. Fluorescent Proteins and Their Applications in Imaging Living Cells and Tissues. Physiol. Rev. 2010, 90, 1103–1163.
6. Stefanachi, A.; Leonetti, F.; Pisani, L.; Catto, M.; Carotti, A. Coumarin: A Natural, Privileged and Versatile Scaffold for Bioactive Compounds. Molecules 2018, 23, 250.
7. Annunziata, F.; Pinna, C.; Dallavalle, S.; Tamborini, L.; Pinto, A. An Overview of Coumarin as a Versatile and Readily Accessible Scaffold with Broad-Ranging Biological Activities. Int. J. Mol. Sci. 2020, 21, 4618.
8. Kumari, R.; Sunil, D.; Ningthoujam, R.S. Naphthalimides in fluorescent imaging of tumor hypoxia—An up-to-date review. Bioorg. Chem. 2019, 88, 102979.
9. Gudeika, D. A review of investigation on 4-substituted 1,8-naphthalimide derivatives. Synth. Met. 2020, 262, 116328.
10. Kamal, A.; Bolla, N.R.; Srikanth, P.S.; Srivastava, A.K. Naphthalimide derivatives with therapeutic characteristics: A patent review. Expert Opin. Ther. Patents 2013, 23, 299–317.
11. Loudet, A.; Burgess, K. BODIPY Dyes and Their Derivatives: Syntheses and Spectroscopic Properties. Chem. Rev. 2007, 107, 4891–4932.
12. Kamkaew, A.; Lim, S.H.; Lee, H.B.; Kiew, L.V.; Chung, L.Y.; Burgess, K. BODIPY dyes in photodynamic therapy. Chem. Soc. Rev. 2013, 42, 77–88.
13. Zhang, W.; Ahmed, A.; Cong, H.; Wang, S.; Shen, Y.; Yu, B. Application of multifunctional BODIPY in photodynamic therapy. Dyes Pigments 2021, 185, 108937.
14. Poddar, M.; Misra, R. Recent advances of BODIPY based derivatives for optoelectronic applications. Co-Ord. Chem. Rev. 2020, 421, 213462.
15. Li, Y.; Zhou, Y.; Yue, X.; Dai, Z. Cyanine Conjugate-Based Biomedical Imaging Probes. Adv. Healthc. Mater. 2020, 9, e2001327.
16. Li, Y.; Zhou, Y.; Yue, X.; Dai, Z. Cyanine conjugates in cancer theranostics. Bioact. Mater. 2021, 6, 794–809.
17. Xiao, Y.; Qian, X. Substitution of oxygen with silicon: A big step forward for fluorescent dyes in life science. Co-Ord. Chem. Rev. 2020, 423, 213513.
18. Rajasekar, M. Recent development in fluorescein derivatives. J. Mol. Struct. 2021, 1224, 129085.
19. Beija, M.; Afonso, C.A.M.; Martinho, J.M.G. Synthesis and applications of Rhodamine derivatives as fluorescent probes. Chem. Soc. Rev. 2009, 38, 2410–2433.
20. Duan, Y.; Liu, M.; Sun, W.; Wang, M.; Liu, S.; Li, Q. Recent Progress on Synthesis of Fluorescein Probes. Mini-Rev. Org. Chem. 2009, 6, 35–43.
21. Castro, R.C.; Ribeiro, D.S.; Santos, D.M.F. Visual detection using quantum dots sensing platforms. Co-Ord. Chem. Rev. 2020, 213637.
22. Shen, C.-L.; Lou, Q.; Liu, K.-K.; Dong, L.; Shan, C.-X. Chemiluminescent carbon dots: Synthesis, properties, and applications. Nano Today 2020, 35, 100954.
23. Poronik, Y.M.; Vygranenko, K.; Gryko, D.; Gryko, D.T. Rhodols—Synthesis, photophysical properties and applications as fluorescent probes. Chem. Soc. Rev. 2019, 48, 5242–5265.
24. Johnson, L.V.; Walsh, M.L.; Chen, L.B. Localization of mitochondria in living cells with rhodamine 123. Proc. Natl. Acad. Sci. USA 1980, 77, 990–994.

25. Urano, Y. Novel live imaging techniques of cellular functions and in vivo tumors based on precise design of small molecule-based ‘Activatable’ fluorescence probes. Curr. Opin. Chem. Biol. 2012, 16, 602–608.

26. Qian, L.; Li, L. Two-photon small molecule enzymatic probes. Acc. Chem. Res. 2016, 49, 626–634.

27. Chen, L.; Li, J.; Du, L.; Li, M. Strategies in the Design of Small-Molecule Fluorescent Probes for Peptidases. Med. Res. Rev. 2014, 34, 1217–1241.

28. Mei, J.; Leung, N.L.C.; Kwok, R.T.K.; Lam, J.W.Y.; Tang, B.Z. Aggregation-Induced Emission: Together We Shine, United We Soar! Chem. Rev. 2015, 115, 11718–11940.

29. Verwilst, P.; Kim, H.S.; Kim, S.; Kang, C.; Kim, J.S. Shedding light on tau protein aggregation: The progress in developing highly selective fluorophores. Chem. Soc. Rev. 2018, 47, 2249–2265.

30. Hou, J.-T.; Ren, W.X.; Li, K.; Seo, J.; Sharma, A.; Yu, X.-Q.; Kim, J.S. Fluorescent bioimaging of pH: From design to applications. Chem. Soc. Rev. 2017, 46, 2076–2090.

31. Fan, J.; Hu, M.; Zhan, P.; Peng, X. Energy transfer cassettes based on organic fluorophores: Construction and applications in ratiometric sensing. Chem. Soc. Rev. 2013, 42, 29–43.

32. Wu, D.; Sedgwick, A.C.; Gunnlaugsson, T.; Akkaya, E.U.; Yoon, J.; James, T.D. Fluorescent chemosensors: The past, present and future. Chem. Soc. Rev. 2017, 46, 7105–7123.

33. Hinckley, D.A.; Seybold, P.G. A spectroscopic/thermodynamic study of the rhodamine B lactone ⇌ zwitterion equilibrium. Spectrochim. Acta Part A Mol. Spectrosc. 1988, 44, 1053–1059.

34. Niu, G.; Liu, W.; Zhou, B.; Xiao, H.; Zhang, H.; Wu, J.; Ge, J.; Wang, P. Deep-Red and Near-Infrared Xanthene Dyes for Rapid Live Cell Imaging. J. Org. Chem. 2016, 81, 7393–7399.

35. Shabir, G.; Saeed, A.; Channar, P.A. A Review on the Recent Trends in Synthetic Strategies and Applications of Xanthene Dyes. Mini-Rev. Org. Chem. 2018, 15, 166–197.

36. Arbeloa, F.L.; Estevez, M.J.T. Photophysics of rhodamines: Molecular structure and solvent effects. J. Phys. Chem. 1991, 95, 2203–2208.

37. Karpiuk, J.; Grabowski, Z.R.; De Schryver, F.C. Photophysics of the Lactone Form of Rhodamine 101. J. Phys. Chem. 1994, 98, 3247–3256.

38. Ramette, R.W.; Sandell, E.B. Rhodamine B Equilibria. J. Am. Chem. Soc. 1956, 78, 4872–4878.

39. Deng, F.; Xu, Z. Heteroatom-substituted rhodamine dyes: Structure and spectroscopic properties. Chin. Chem. Lett. 2019, 30, 1667–1681.

40. Wang, L.; Du, W.; Hu, Z.; Uvdal, K.; Li, L.; Huang, W. Hybrid Rhodamine Fluorophores in the Visible/NIR Region for Biological Imaging. Angew. Chem. Int. Ed. 2019, 58, 14026–14043.

41. Koide, Y.; Urano, Y.; Hanaoka, K.; Terai, T.; Nagano, T. Development of an Si-Rhodamine-Based Far-Red to Near-Infrared Fluorescence Probe Selective for Hypochlorous Acid and Its Applications for Biological Imaging. J. Am. Chem. Soc. 2011, 133, 5680–5682.

42. Uno, S.-N.; Kamiya, M.; Yoshihara, T.; Sugawara, K.; Okabe, K.; Tarhan, M.C.; Fujita, H.; Funatsu, T.; Okada, Y.; Tobita, S.; et al. A spontaneously blinking fluorophore based on intramolecular spirocyclization for live-cell super-resolution imaging. Nat. Chem. 2014, 6, 681–689.

43. Sakabe, M.; Asanuma, D.; Kamiya, M.; Iwatate, R.J.; Hanaoka, K.; Terai, T.; Nagano, T.; Urano, Y. Rational Design of Highly Sensitive Fluorescence Probes for Protease and Glycosidase Based on Precisely Controlled Spirocyclization. J. Am. Chem. Soc. 2013, 135, 409–414.

44. Tachibana, R.; Kamiya, M.; Suzuki, S.; Morokuma, K.; Nanjo, A.; Urano, Y. Molecular design strategy of fluorogenic probes based on quantum chemical prediction of intramolecular spirocyclization. Commun. Chem. 2020, 3, 82.

45. Tachibana, R.; Kamiya, M.; Morozumi, A.; Miyazaki, Y.; Fujioka, H.; Nanjo, A.; Kojima, R.; Komatsu, T.; Ueno, T.; Hanaoka, K.; et al. Design of spontaneously blinking fluorophores for live-cell super-resolution imaging based on quantum-chemical calculations. Chem. Commun. 2020, 56, 13173–13176.

46. Zhu, W.; Chai, X.; Wang, B.; Zou, Y.; Wang, T.; Meng, Q.; Wu, Q. Spiroboronate Si-rhodamine as a near-infrared probe for imaging lysosomes based on the reversible ring-opening process. Chem. Commun. 2015, 51, 9608–9611.

47. Uno, S.-N.; Kamiya, M.; Morozumi, A.; Urano, Y. A green-light-emitting, spontaneously blinking fluorophore based on intramolecular spirocyclization for dual-colour super-resolution imaging. Chem. Commun. 2018, 54, 102–105.

48. Méndez-Ardoy, A.; Reina, J.J.; Montenegro, J. Synthesis and Supramolecular Functional Assemblies of Ratiometric pH Probes. Chem. Eur. J. 2020, 26, 7516–7536.

49. Nath, S.; Saad, M.A.; Pigula, M.; Swain, J.W.; Hasan, T. Photoimmunotherapy of Ovarian Cancer: A Unique Niche in the Management of Advanced Disease. Cancers 2019, 11, 1887.
50. Grimm, J.B.; Sung, A.J.; Legant, W.R.; Hulamm, P.; Matlosz, S.M.; Betzig, E.; Lavis, L.D. Carbofluoresceins and Carborhodamines as Scaffolds for High-Contrast Fluorogenic Probes. ACS Chem. Biol. 2013, 8, 1303–1310.
51. Grimm, J.B.; Tkachuk, A.N.; Xie, L.; Choi, H.; Mohar, B.; Falco, N.; Schaefer, K.; Patel, R.; Zheng, Q.; Liu, Z.; et al. A general method to optimize and functionalize red-shifted rhodamine dyes. Nat. Methods 2020, 17, 815–821.
52. Grimm, J.B.; Muthusamy, A.K.; Liang, Y.; Brown, T.A.; Lemon, W.C.; Patel, R.; Lu, R.; Macklin, J.J.; Keller, P.J.; Yajie, L.; et al. A general method to fine-tune fluorophores for live-cell and in vivo imaging. Nat. Methods 2017, 14, 987–994.
53. Wang, L.; Frei, M.S.; Salim, A.; Johnsson, K. Small-Molecule Fluorescent Probes for Live-Cell Super-Resolution Microscopy. J. Am. Chem. Soc. 2019, 141, 2770–2781.
54. Jia, S.; Ramos-Torres, K.M.; Kolemen, S.; Ackerman, C.M.; Chang, C.J. Tuning the Color Palette of Fluorescent Copper Sensors through Systematic Heteroatom Substitution at Rhodol Cores. ACS Chem. Biol. 2018, 13, 1844–1852.
55. Wang, S.; Li, B.; Zhang, F. Molecular Fluorophores for Deep-Tissue Bioimaging. ACS Cent. Sci. 2020, 6, 1302–1316.
56. Sasaki, S.; Drummen, G.P.C.; Konishi, G.-I. Recent advances in twisted intramolecular charge transfer (TICT) fluorescence and related phenomena in materials chemistry. J. Mater. Chem. C 2016, 4, 2731–2743.
57. Pantazis, A.; Westerberg, K.; Althoff, T.; Abramson, J.; Olcese, R. Harnessing photoinduced electron transfer to optically determine protein sub-nanoscale atomic distances. Nat. Commun. 2018, 9, 4738.
58. Daly, B.; Ling, J.; De Silva, A.P. Current developments in fluorescent PET (photoinduced electron transfer) sensors and switches. Chem. Soc. Rev. 2015, 44, 4203–4211.
59. Feng, S.; Gong, S.; Feng, G. Aggregation-induced emission and solid fluorescence of fluorescein derivatives. Chem. Commun. 2020, 56, 2511–2513.
60. Liu, H.-W.; Chen, L.; Xu, C.; Li, Z.; Zhang, H.; Zhang, X.-B.; Tan, W. Recent progresses in small-molecule enzymatic fluorescent probes for cancer imaging. Chem. Soc. Rev. 2018, 47, 7140–7180.
61. Hanash, S.M. Disease proteomics. Nat. Cell Biol. 2003, 422, 226–232.
62. MacDougall, J.R.; Matrisian, L.M. Contributions of tumor and stromal matrix metalloproteinases to tumor progression, invasion and metastasis. Cancer Metastasis Rev. 1995, 14, 351–362.
63. Thiry, A.; Dogné, J.-M.; Masereel, B.; Supuran, C.T. Targeting tumor-associated carbonic anhydrase IX in cancer therapy. Trends Pharmacol. Sci. 2006, 27, 566–573.
64. Copeland, R.A.; Harpel, M.R.; Tummino, P.J. Targeting enzyme inhibitors in drug discovery. Expert Opin. Ther. Targets 2007, 11, 967–978.
65. Wolf, P.L. Clinical significance of serum high-molecular-mass alkaline phosphatase, alkaline phosphatase—Lipoprotein-X complex, and intestinal variant alkaline phosphatase. J. Clin. Lab. Anal. 1994, 8, 172–176.
66. Chatterjee, S.K.; Bhattacharya, M.; Barlow, J.J. Glycosyltransferase and glycosidase activities in ovarian cancer patients. Cancer Res. 1979, 39, 1943–1951.
67. Zhang, J.; Chai, X.; He, X.-P.; Kim, H.-J.; Yoon, J.; Tian, H. Fluorogenic probes for disease-relevant enzymes. Chem. Soc. Rev. 2019, 48, 683–722.
68. Li, M.; Yuan, L.; Chen, Y.; Ma, W.; Ran, F.; Zhang, L.; Zhou, D.; Xiao, S. Rhodamine B-based fluorescent probes for molecular mechanism study of the anti-influenza activity of pentacyclic triterpenes. Eur. J. Med. Chem. 2020, 205, 112664.
69. Iii, J.R.Y.; Gilchrist, A.; Howell, K.E.; Bergeron, J.J.M. Proteomics of organelles and large cellular structures. Nat. Rev. Mol. Cell Biol. 2005, 6, 702–714.
70. Johnson, T.A.; Jinnah, H.A.; Kamatani, N. Shortage of Cellular ATP as a Cause of Diseases and Strategies to Enhance ATP. Front. Pharmacol. 2019, 10, 98.
71. Song, Y.; Zheng, Y.; Zhang, S.; Song, Y.; Niu, M.; Li, Y.; Ye, Z.; Yu, H.; Zhang, M.; Xiao, Y. Always-on and water-soluble rhodamine amide designed by positive charge effect and application in mitochondrion-targetable imaging of living cells. Sens. Actuators B Chem. 2019, 286, 32–38.
72. Kim, H.N.; Lee, M.H.; Kim, H.J.; Kim, J.S.; Yoon, J. A new trend in rhodamine-based chemosensors: Application of spirolactam ring-opening to sensing ions. Chem. Soc. Rev. 2008, 37, 1465–1472.
73. Huang, C.-Y.; Ju, D.-T.; Chang, C.-F.; Reddy, P.M.; Velmurugan, B.K. A review on the effects of current chemotherapy drugs and natural agents in treating non-small cell lung cancer. Biomedicine 2017, 7, 23.

74. Vasan, N.; Baselga, J.; Hyman, D.M. A view on drug resistance in cancer. Nat. Cell Biol. 2019, 575, 299–309.

75. Rosenberg, B.H.; Vancamp, L.; Trosko, J.E.; Mansour, V.H. Platinum Compounds: A New Class of Potent Antitumour Agents. Nat. Cell Biol. 1969, 222, 385–386.

76. Wang, X.; Lin, J.; Zhang, X.; Liu, Q.; Xu, Q.; Tan, R.; Guo, Z. 5-Fluorouracil-cisplatin adducts with potential antitumor activity. J. Inorg. Biochem. 2003, 94, 186–192.

77. Wang, X.; Guo, Z. Targeting and delivery of platinum-based anticancer drugs. Chem. Soc. Rev. 2013, 42, 202–224.

78. Xu, Z.; Kong, D.; He, X.; Guo, L.; Ge, X.; Liu, X.; Zhang, H.; Li, J.; Yang, Y.; Liu, Z. Mitochondria-targeted half-sandwich rutheniumII diimine complexes: Anticancer and antimetastasis via ROS-mediated signalling. Inorg. Chem. Front. 2018, 5, 2100–2105.

79. Mao, Z.-W.; Liehr, G.; Heinemann, F.W.; Van Eldik, R. Complex-formation reactions of Cu(II) and Zn(II) 2,2′-bipyridine and 1,10-phenanthroline complexes with bicarbonate. Identification of different carbonate coordination modes. J. Chem. Soc. Dalton Trans. 2001, 2, 3652–3662.

80. Oun, R.; Moussa, Y.E.; Wheate, N.J. The side effects of platinum-based chemotherapy drugs: A review for chemists. Dalton Trans. 2018, 47, 6645–6653.

81. Guan, R.; Chen, Y.; Zeng, L.; Rees, T.W.; Jin, C.; Huang, J.; Chen, Z.-S.; Ji, L.; Chao, H. Oncosis-inducing cyclometalated iridium(iii) complexes. Chem. Sci. 2018, 9, 5183–5190.

82. Chao, H.; Chen, L.; Rees, T.W.; Chen, Y.; Liu, J.; Ji, L.-N.; Long, J.; Chao, H. A mitochondria-targeting hetero-binuclear Ir(iii)-Pt(ii) complex induces necrosis in cisplatin-resistant tumor cells. Chem. Commun. 2018, 54, 6268–6271.

83. Gasser, G.; Ott, I.; Metzler-Nolte, N. Organometallic Anticancer Compounds. J. Med. Chem. 2011, 54, 3–25.

84. He, L.; Tan, C.-P.; Ye, R.-R.; Zhao, Y.-Z.; Liu, Y.-H.; Zhao, Q.; Ji, L.-N.; Mao, Z. Theranostic Iridium(III) Complexes as One- and Two-Photon Phosphorescent Trackers to Monitor Autophagic Lysosomes. Angew. Chem. Int. Ed. 2014, 53, 12137–12141.

85. Liu, Z.; Guo, L.; Tian, Z.; Tian, M.; Zhang, S.; Xu, Z.; Gong, P.; Zheng, X.-F.; Zhao, J.; Liu, Z. Significant effects of counteranions on the anticancer activity of iridium(iii) complexes. Chem. Commun. 2018, 54, 4421–4424.

86. Zhang, P.; Chiu, C.K.C.; Huang, H.; Lam, Y.P.Y.; Habtemariam, A.; Malcomson, T.; Paterson, M.J.; Clarkson, G.J.; O'Connor, P.B.; Chao, H.; et al. Organoiridium Photosensitizers Induce Specific Oxidative Attack on Proteins within Cancer Cells. Angew. Chem. Int. Ed. 2017, 56, 14898–14902.

87. Liu, Z.; Deliang, K.; Zhang, S.; Guo, L.; He, X.; Kong, D.; Zhang, H.; Liu, Z. Half-sandwich ruthenium(ii) complexes containing N^N-chelated imino-pyridyl ligands that are selectively toxic to cancer cells. Chem. Commun. 2017, 53, 12810–12813.

88. Li, J.; Tian, M.; Tian, Z.; Zhang, S.; Yan, C.; Shao, C.; Liu, Z. Half-Sandwich Iridium(III) and Ruthenium(II) Complexes Containing P^P-Chelating Ligands: A New Class of Potent Anticancer Agents with Unusual Redox Features. Inorg. Chem. 2018, 57, 1705–1716.

89. Leist, M.; Jäättelä, M. Triggering of apoptosis by cathepsins. Cell Death Differ. 2001, 8, 324–326.

90. Guicciardi, M.E.; Leist, M.; Gores, G. Lysosomes in cell death. Oncogene 2004, 23, 2881–2890.

91. Ma, W.; Tian, Z.; Zhang, S.; He, X.; Li, J.; Xia, X.; Chen, X.; Liu, Z. Lysosome targeted drugs: Rhodamine B modified N^N-chelating ligands for half-sandwich iridium(iii) anticancer complexes. Inorg. Chem. Front. 2018, 5, 2587–2597.

92. Gutscher, M.; Pauleau, A.-L.; Marty, L.; Brach, T.; Wabnitz, G.H.; Samstag, Y.; Meyer, A.J.; Dick, T.P. Real-time imaging of the intracellular glutathione redox potential. Nat. Methods 2008, 5, 553–559.

93. Forman, H.J.; Zhang, H.; Rinna, A. Glutathione: Overview of its protective roles, measurement, and biosynthesis. Mol. Asp. Med. 2009, 30, 1–12.

94. Szabo, C. Gasotransmitters in cancer: From pathophysiology to experimental therapy. Nat. Rev. Drug Discov. 2016, 15, 185–203.

95. Wierzbicki, A.S. Homocysteine and cardiovascular disease: A review of the evidence. Diabetes Vasc. Dis. Res. 2007, 4, 143–149.

96. Das, J.R.; Kaul, S. Homocysteine and Cardiovascular Disease. In Glutathione and Sulfur Amino Acids in Human Health and Disease; John Wiley & Sons, Inc.: Hoboken, NJ, USA, 2008; pp. 413–439. ISBN 9780470170854.

97. Dai, J.; Ma, C.; Zhang, P.; Fu, Y.; Shen, B.-X. Recent progress in the development of fluorescent probes for detection of biothiols. Dyes Pigments 2020, 177, 108321.

98. Tong, L.L.; Qian, Y. A NIR rhodamine fluorescent chemodosimeter specific for glutathione: Knoevenagel condensation, detection of intracellular glutathione and living cell imaging. J. Mater. Chem. B 2018, 6, 1791–1798.

99. Möckl, L.; Lamb, D.C.; Bräuchle, C. Super-resolved Fluorescence Microscopy: Nobel Prize in Chemistry 2014 for Eric Betzig, Stefan Hell, and William E. Moerner. Angew. Chem. Int. Ed. 2014, 53, 13972–13977.

100. Vangindertael, J.; Camacho, R.; Sempels, W.; Mizuno, H.; Dedecker, P.; Janssen, K.P.F. An introduction to optical super-resolution microscopy for the adventurous biologist. Methods Appl. Fluoresc. 2018, 6, 022003.

101. Pujals, S.; Feiner-Gracia, N.; Delcanale, P.; Voets, I.; Albertazzi, L. Super-resolution microscopy as a powerful tool to study complex synthetic materials. Nat. Rev. Chem. 2019, 3, 68–84.

102. Sharma, R.; Singh, M.; Sharma, R. Recent advances in STED and RESOLFT super-resolution imaging techniques. Spectrochim. Acta Part A Mol. Biomol. Spectrosc. 2020, 231, 117715.

103. Blom, H.; Widengren, J. Stimulated Emission Depletion Microscopy. Chem. Rev. 2017, 117, 7377–7427.

104. Hess, S.T.; Girirajan, T.P.K.; Mason, M.D. Ultra-High Resolution Imaging by Fluorescence Photoactivation Localization Microscopy. Biophys. J. 2006, 91, 4258–4272.

105. Betzig, E.; Patterson, G.H.; Sougrat, R.; Lindwasser, O.W.; Olenych, S.; Bonifacino, J.S.; Davidson, M.W.; Lippincott-Schwartz, J.; Hess, H.F. Imaging Intracellular Fluorescent Proteins at Nanometer Resolution. Science 2006, 313, 1642–1645.

106. Xu, J.; Ma, H.; Liu, Y. Stochastic Optical Reconstruction Microscopy (STORM). Curr. Protoc. Cytom. 2017, 81, 12.46.1–12.46.27.

107. Khater, I.M.; Nabi, I.R.; Hamarneh, G. A Review of Super-Resolution Single-Molecule Localization Microscopy Cluster Analysis and Quantification Methods. Gene Expr. Patterns 2020, 1, 100038.

108. He, H.; Ye, Z.; Zheng, Y.; Xu, X.; Guo, C.; Xiao, Y.; Yang, W.; Qian, X.; Yang, Y. Super-resolution imaging of lysosomes with a nitroso-caged rhodamine. Chem. Commun. 2018, 54, 2842–2845.

109. Wysocki, L.M.; Lavis, L.D. Advances in the chemistry of small molecule fluorescent probes. Curr. Opin. Chem. Biol. 2011, 15, 752–759.

110. Adams, S.R.; Tsien, R.Y. Controlling Cell Chemistry with Caged Compounds. Annu. Rev. Physiol. 1993, 55, 755–784.

111. Fernández-Suárez, M.; Ting, A.Y. Fluorescent probes for super-resolution imaging in living cells. Nat. Rev. Mol. Cell Biol. 2008, 9, 929–943.

112. Banala, S.; Maurel, D.; Manley, S.; Johnsson, K. A Caged, Localizable Rhodamine Derivative for Superresolution Microscopy. ACS Chem. Biol. 2011, 7, 289–293.

113. Klán, P.; Šolomek, T.; Bochet, C.G.; Blanc, A.; Givens, R.; Rubina, M.; Popik, V.; Kostikov, A.; Wirz, J. Photoremovable Protecting Groups in Chemistry and Biology: Reaction Mechanisms and Efficacy. Chem. Rev. 2013, 113, 119–191.

114. Bucevičius, J.; Kostiuk, G.; Gerasimaitė, R.; Gilat, T.; Lukinavičius, G. Enhancing the biocompatibility of rhodamine fluorescent probes by a neighbouring group effect. Chem. Sci. 2020, 11, 7313–7323.

115. Van De Linde, S.; Heilemann, M.; Sauer, M. Live-Cell Super-Resolution Imaging with Synthetic Fluorophores. Annu. Rev. Phys. Chem. 2012, 63, 519–540.

116. Lukinavičius, G.; Mitronova, G.Y.; Schnorrenberg, S.; Butkevich, A.N.; Barthel, H.; Belov, V.N.; Hell, S.W. Fluorescent dyes and probes for super-resolution microscopy of microtubules and tracheoles in living cells and tissues. Chem. Sci. 2018, 9, 3324–3334.

117. Lukinavičius, G.; Reymond, L.; Umezawa, K.; Sallin, O.; D'Este, E.; Goettfert, F.; Ta, H.; Hell, S.W.; Urano, Y.; Johnsson, K. Fluorogenic Probes for Multicolor Imaging in Living Cells. J. Am. Chem. Soc. 2016, 138, 9365–9368.

118. Butkevich, A.N.; Mitronova, G.Y.; Sidenstein, S.C.; Klocke, J.L.; Kamin, D.; Meineke, D.N.H.; D'Este, E.; Kraemer, P.-T.; Danzl, J.G.; Belov, V.N.; et al. Fluorescent Rhodamines and Fluorogenic Carbopyronines for Super-Resolution STED Microscopy in Living Cells. Angew. Chem. Int. Ed. 2016, 55, 3290–3294.

119. Wang, L.; Tran, M.; D'Este, E.; Roberti, J.; Koch, B.; Xue, L.; Johnsson, K. A general strategy to develop cell permeable and fluorogenic probes for multicolour nanoscopy. Nat. Chem. 2020, 12, 165–172.

120. Butkevich, A.N.; Belov, V.N.; Kolmakov, K.; Sokolov, V.V.; Shojaei, H.; Sidenstein, S.C.; Kamin, D.; Matthias, J.; Vlijm, R.; Engelhardt, J.; et al. Hydroxylated Fluorescent Dyes for Live-Cell Labeling: Synthesis, Spectra and Super-Resolution STED. Chem. Eur. J. 2017, 23, 12114–12119.

121. Zheng, Q.; Ayala, A.X.; Chung, I.; Weigel, A.V.; Ranjan, A.; Falco, N.; Grimm, J.B.; Tkachuk, A.N.; Wu, C.; Lippincott-Schwartz, J.; et al. Rational Design of Fluorogenic and Spontaneously Blinking Labels for Super-Resolution Imaging. ACS Cent. Sci. 2019, 5, 1602–1613.

122. Teh, E.-J.; Leong, Y.; Liu, Y. Isomerism and Solubility of Benzene Mono- and Dicarboxylic Acid: Its Effect on Alumina Dispersions. Langmuir 2011, 27, 49–58.

123. Maeda, S.; Harabuchi, Y.; Ono, Y.; Taketsugu, T.; Morokuma, K. Intrinsic reaction coordinate: Calculation, bifurcation, and automated search. Int. J. Quantum Chem. 2015, 115, 258–269.